Rapid cell-cycle reentry and cell death after acute inactivation of the retinoblastoma gene product in postnatal cochlear hair cells

Thomas Weber*, Mary K. Corbett*, Lionel M. L. Chow*, Marcus B. Valentine†, Suzanne J. Baker*, and Jian Zuo*‡

Departments of *Developmental Neurobiology and †Genetics and Tumor Cell Biology, St. Jude Children's Research Hospital, Memphis, TN 38105

Edited by Kathryn V. Anderson, Sloan–Kettering Institute, New York, NY, and approved November 28, 2007 (received for review August 26, 2007)

Unlike lower vertebrates, mammals are unable to replace damaged mechanosensory hair cells (HCs) in the cochlea. Recently, ablation of the retinoblastoma protein (Rb) in undifferentiated mouse HC precursors was shown to cause cochlear HC proliferation and the generation of new HCs, raising the hope that inactivation of Rb in postmitotic HCs could trigger cell division and regenerate functional HCs postnatally. Here, we acutely inactivated Rb in nearly all cochlear HCs of newborn mice, using a newly developed HC-specific inducible Cre mouse line. Beginning 48 h after *Rb* deletion, ≈40% of HCs were in the S and M phases of the cell cycle, demonstrating an overriding role for Rb in maintaining the quiescent state of postnatal HCs. Unlike *Rb*-null HC precursors, such HCs failed to undergo cell division and died rapidly. HC clusters were restricted to the less differentiated cochlear regions, consistent with differentiation-dependent roles of Rb. Moreover, outer HCs expressed the maturation marker prestin, suggesting an embryonic time window for Rb-dependent HC specification. We conclude that Rb plays essential and age-dependent roles during HC proliferation and differentiation, and, in contrast to previous hypotheses, cell death after forced cell-cycle reentry presents a major challenge for mammalian HC regeneration from residual postnatal HCs.

prestin | regeneration

Cochlear hair cells (HCs) in the mammalian inner ear are mechanosensory receptors that transduce sound into electrical signals. HCs and their surrounding supporting cells (SCs) derive from common precursors during the embryonic development of the inner ear. In mice, these progenitors exit the cell cycle approximately on embryonic days (E)13–14 and become quiescent (1–3). Permanent cell-cycle exit is followed by differentiation into SCs and HCs later in embryonic development and functional subdifferentiation into inner and outer HCs (IHCs and OHCs) postnatally (reviewed in ref. 4).

Genetic and environmental factors, such as noise and ototoxic drugs, can damage HCs, leading to their death and to permanent hearing loss. Mammalian HCs are not regenerated, whereas nonmammalian vertebrates are able to replenish lost sensory HCs by proliferation and differentiation of nearby SCs within the sensory epithelium (5–7). The critical difference in the regenerative ability of mammalian cochleae and nonmammalian hearing organs appears to be their proliferative responsiveness after trauma.

A key inhibitor of proliferation is the retinoblastoma protein (Rb), a member of the family of pocket domain proteins. These proteins bind to E2F transcription factors and can repress genes required during the S phase, thereby maintaining cells in a quiescent state (reviewed in ref. 8). Rb is expressed in embryonic and postnatal HCs; its absence in HC precursors of mice led to the production of supernumerary HCs that appeared functional, demonstrating that mammalian HC precursors can indeed be manipulated to proliferate (9, 10). However, HC injury typically occurs after birth; our aim was therefore to determine whether the inactivation of Rb could trigger cell-cycle reentry in postnatal HCs. The consequences of Rb loss *in vivo* have been studied in many tissues, using mouse models (11); in this study, we inactivated Rb in postnatal HCs, using a newly developed tamoxifen-inducible Cre mouse line. We observed that HCs rapidly reentered the cell cycle after the loss of Rb but died without generating supernumerary HCs. Thus, forced cell-cycle reentry by Rb inactivation had an entirely different outcome in postnatal HCs than in embryonic precursor cells for HCs and SCs, having limited use for hair cell regeneration.

Results

Inducible Inactivation of Rb Function in Postnatal Cochlear HCs. We used the Cre-*loxP* system (12) to ablate Rb function in postmitotic HCs. A gene-targeted mouse ($Rb^{lox/lox}$) with exon 19 of the *Rb* gene flanked by two *loxP* sites (13) was crossed with the *Atoh1-CreER*^{TM} mice that exhibited inducible Cre activity specifically in nearly all cochlear HCs when injected with tamoxifen once a day on postnatal days (P) 0 and P1 [unless stated otherwise; Fig. 1 and refs. 14 and 15]. The mice used were tamoxifen-injected *Atoh1-CreER*^{TM}:$Rb^{lox/lox}$ (designated $Rb^{-/-}$), *Atoh1-CreER*^{TM}:$Rb^{+/lox}$ ($Rb^{+/-}$), and *Atoh1-CreER*^{TM}-negative:$Rb^{lox/lox}$ mice ($Rb^{lox/lox}$) mice. Among the offspring, three possible *Rb* alleles—wild-type, floxed (unrecombined), and inactivated (recombined)—were confirmed subsequently by PCR, using genomic DNA extracted from the cochlea (Fig. 1*A*). To determine the onset of Cre activity, we administered a single tamoxifen injection on P0 and observed recombination after 30 h but not after 6, 12, 18, or 24 h (Fig. 1*B*). Therefore, the time required for the absorption of tamoxifen, translocation of *CreER*^{TM} recombinase into the nucleus, and efficient recombination in HCs is between 24 and 30 h after injections on P0. We did not observe phenotypes in $Rb^{+/-}$ mice or in most other tissues, and mice of all genotypes survived well into adulthood (data not shown; see ref. 14).

Rapid HC Loss upon Acute Inactivation of Rb. To determine whether postmitotic HCs proliferate in the absence of Rb, we dissected cochleae from $Rb^{-/-}$ and $Rb^{+/-}$ mice. On P3, confocal scans of cochlear whole mounts stained with HC markers revealed a wild-type-like morphology of the organ of Corti in all genotypes (Fig. 2 *A* and *B*). These findings underlined that, until P3, $Rb^{-/-}$ HCs had undergone normal development, including regular cell-cycle exit.

When HC numbers were analyzed in cochlear whole mounts after P3, we found that IHC and OHC numbers in $Rb^{-/-}$ mice decreased rapidly between P4 and P15 relative to those in $Rb^{+/-}$ mice, without signs of additional HCs at any stage (Fig. 2). By

Author contributions: T.W., S.J.B., and J.Z. designed research; T.W., M.K.C., L.M.L.C., and M.B.V. performed research; S.J.B. contributed new reagents/analytic tools; T.W., M.K.C., L.M.L.C., M.B.V., S.J.B., and J.Z. analyzed data; and T.W. and J.Z. wrote the paper.

The authors declare no conflict of interest.

This article is a PNAS Direct Submission.

‡To whom correspondence should be addressed. E-mail: jian.zuo@stjude.org.

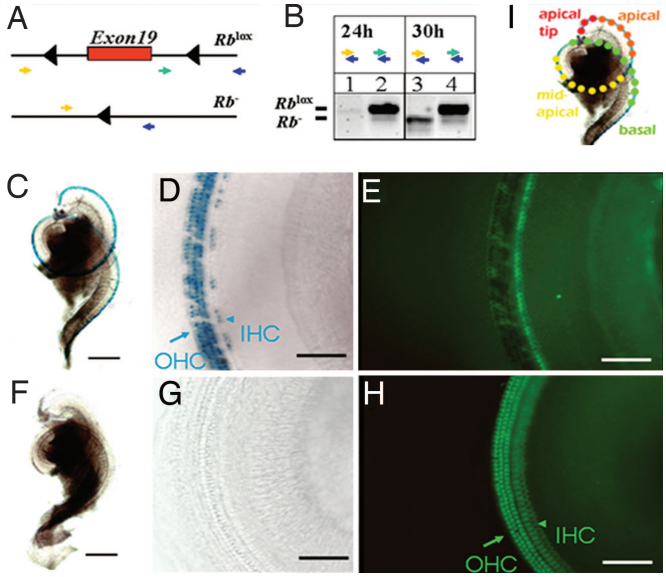

Fig. 1. Inducible recombination of the *Rb* gene locus. (*A*) Two targeted *Rb* alleles. Exon 19 of *Rb* is flanked by two unrecombined *lox*P sites (black triangles; Rb^{lox} in *B Lower*). Cre-mediated deletion of exon 19 results in an allele encoding a nonfunctional Rb protein (Rb^{-} in *B Lower*). Two combinations of PCR genotyping primer pairs were used to distinguish the Rb^{lox} allele (283-bp band from the green and blue pair) from the Rb^{-} allele (260-bp band from the yellow and blue pair). (*B*) PCR analysis, using cochlear genomic DNA of *Atoh1-CreER:* $Rb^{lox/lox}$ mice given injections on P0. The primer combination used for each lane is indicated. The Rb^{-} band was not detected after 24 h (lane 1), but it was detected after 30 h (lane 3). The corresponding Rb^{lox} bands from unrecombined cells are shown as controls (lanes 2 and 4). (*C–H*) Cre activity within the cochlea as visualized by lacZ staining. The mice were given injections on P0 and P1 and analyzed on P6. (*C* and *F*) LacZ-positive (blue) staining of cochlear whole mounts from *Atoh1-CreER*: *Rosa26* mice given tamoxifen injections (*C*) and mock injections (*F*). (*D* and *G*). Higher magnification reveals that Cre-activity was limited to OHCs (arrow) and IHCs (arrowhead) (blue, lacZ staining in *D*), whereas no lacZ staining was detected in mice given mock injections (*G*). (*E* and *H*) Myosin7a (green) coimmunostaining of regions in *D* and *G* reveals the presence of HCs. Note that fluorescence is masked in cells that express lacZ (*E* compared with *H*). [Scale bars: *C*, 0.25 mm (applies to *C* and *F*); and *D*, 80 μm (applies to *D*, *E*, *G*, and *H*)]. Note that ≈80% of IHCs and ≈90% of OHCs were lacZ-positive when induced at P0 and P1 under these conditions (14). (*I*) Illustration of HCs and their locations in different regions within a cochlear whole mount from basal (green dots) to apical (red dots). The apical tip contained the least differentiated HCs at the times analyzed in this study (P4–P6 and P9), whereas the basal HCs were more mature. Consistently, in subsequent figures (unless stated otherwise), arrows denote OHCs, and arrowheads denote IHCs.

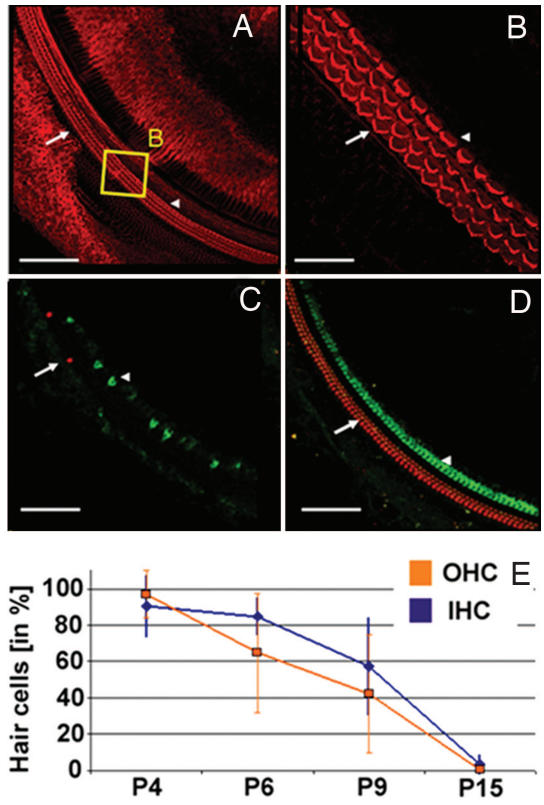

Fig. 2. HC loss in $Rb^{-/-}$ mice. (*A*) Confocal *z* projections reveal the normal morphology of an $Rb^{-/-}$ cochlear whole mount on P3 after tamoxifen injection on P0 and P1. [Scale bar, 100 μm (refers to *A*, *C* and *D*)]. Phalloidin staining (red). Arrows indicate OHCs; arrowheads indicate IHCs. (*B*) The region in the yellow box in *A* at a higher magnification allows the visualization of the orderly stereocilia (V-shapes) of OHCs (three rows) and IHCs (one row). (Scale bar, 20 μm.) (*C*) On P15 $Rb^{-/-}$ mice display a severe loss of IHCs and OHCs. Prestin (red) and myosin7a (green). (*D*) $Rb^{+/-}$ littermates exhibit no cochlear abnormalities on P15. (*E*) Progressive loss of OHCs (blue) and IHCs (orange) from P4 to P15 in $Rb^{-/-}$ mice. Surviving HCs in $Rb^{-/-}$ mice were normalized to those in $Rb^{+/-}$ littermates at corresponding ages and are depicted as a percentage of $Rb^{-/-}/Rb^{+/-}$. Curves were fitted by using linear regression of mean values. Error bars indicate standard deviations. The number of cochlear regions in at least three mice analyzed and statistical significance ($Rb^{-/-}$ vs. $Rb^{+/-}$, Student's *t* test) are as follows: on P4, IHCs, $n = 7$ ($P > 0.05$), and OHCs, $n = 8$ ($P > 0.05$); on P6, IHCs, $n = 7$ ($P < 0.01$), and OHCs, $n = 5$ ($P < 0.05$); on P9, IHCs, $n = 12$ ($P < 0.01$), and OHCs, $n = 12$ ($P < 0.01$); and on P15, IHCs, $n = 6$ ($P < 0.01$), and OHCs, $n = 6$ ($P < 0.01$).

P15, nearly all HCs were lost in $Rb^{-/-}$ mice, whereas $Rb^{+/-}$ littermates had a normal organ of Corti without HC loss at all ages, indicating that one copy of *Rb* is sufficient to maintain quiescence and survival of postmitotic HCs (Fig. 2*D*). Furthermore, it can be deduced that after the recombination of the *Rb* gene locus, turnover of endogenous Rb in HCs and subsequent processes leading to HC loss span a period of 2–3 days. Consistently, when tested after 6 weeks, using click auditory brainstem responses, all $Rb^{-/-}$ mice displayed profound hearing loss [thresholds >85 sound pressure level (dB SPL), $n = 7$], whereas $Rb^{+/-}$ and $Rb^{lox/lox}$ mice had normal hearing (thresholds ≈25 dB SPL, $n = 11$ and 2, respectively) (data not shown; procedures are described in ref. 16).

Rapid Cell-Cycle Reentry and Cell Death of Postmitotic HCs. To investigate whether postmitotic HCs would reenter the cell cycle upon acute loss of Rb function, we gave mice i.p. injections of 5-bromo-2′-deoxyuridine and 5-fluoro-2′-deoxyuridine (BrdU) on P4 every 2 h for five consecutive doses and analyzed them 12 h after the first injection. Cells entering the S phase within 12 h on P4 and thus incorporating BrdU into replicated DNA should have been detectable by using anti-BrdU immunostaining. In $Rb^{+/-}$ littermates, no BrdU-positive HC nuclei were detected (Fig. 3*A*), whereas ≈40% of the HC nuclei in $Rb^{-/-}$ mice were BrdU-positive (Fig. 3*B*). Such nuclei appeared in basal and apical cochlear turns at similar rates (data not shown). Their high percentage within a 12 h time window, 4 days after the first tamoxifen injection and 2–3 days after the recombination of the *Rb* gene locus, indicated a synchronized S phase entry of HCs. BrdU-positive cells within the organ of Corti were costained with the HC marker myosin7a, indicating that no cell-cycle reentry of SCs had occurred.

Changes in chromatin conformation at the onset of the M phase involve the phosphorylation of histone H3. Antibodies against phosphorylated Ser-10 of histone H3 stained the nuclei in HCs of $Rb^{-/-}$ mice (Fig. 3*C*) but not in those of $Rb^{+/-}$ littermates on P5 (data not shown). Consistently, changes in

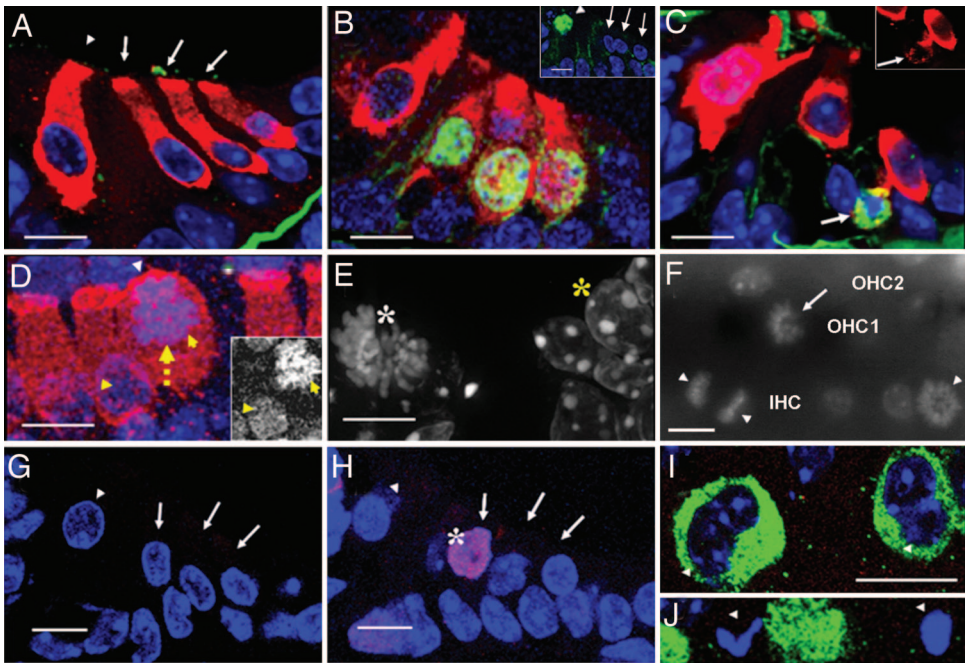

Fig. 3. $Rb^{-/-}$ HCs in the S and M phases of the cell cycle and undergoing cell death. (*A–C*) Confocal images of sections through the organ of Corti, myosin7a immunostaining marks HCs (red, myosin7a; blue, DAPI). (*A* and *B*) Overlay in a BrdU pulse-labeling experiment on P4 (green, BrdU). (*A*) No BrdU staining in HC nuclei of $Rb^{+/-}$ mice (none of 597 HCs, $n = 3$). Basilar membrane staining is background. Arrows indicate OHCs; the arrowhead indicates IHC. (*B*) Strong BrdU staining in three OHC nuclei of $Rb^{-/-}$ mice. A total of 261 of 659 HCs (39.6%) and no SC nuclei were BrdU-positive ($n = 2$). Staining of myosin7a in the nucleus of the OHC at the right might indicate disruption of the nuclear envelope and the beginning of cell death. (*Inset*) BrdU labeling of an IHC (green, arrowhead) of a basal turn cochlear section at P4; this cell is presumed IHC because of its expression of myosin7a (data not shown) and its position. (*C*) Phosphorylated histone H3 labeling (green, arrow) of $Rb^{-/-}$ OHCs on P5. (*Inset*) myosin7a staining (red channel only) of the same cell (the arrow indicates positive for phosphorylated histone H3), demonstrating that it is an HC. (*D*) Confocal whole-mount *z* projection of $Rb^{-/-}$ IHCs. Blue, DAPI; red, myosin7a. The yellow arrow indicates nuclear migration from the basal to the apical pole of the cell. Yellow arrowheads indicate migrating and normal nuclei of IHCs. The white arrowhead indicates the intact cuticular plate at the apical pole. (*Inset*) DAPI channel (in gray) of the same IHC nuclei marked with yellow arrowheads. (*E*) High-resolution deconvoluted fluorescence image of a basal $Rb^{-/-}$ HC nucleus on P5 stained with DAPI (white asterisk); individual chromosomes in metaphase can be seen. Adjacent interphase nuclei are shown for comparison (yellow asterisk). (*F*) DAPI (gray) fluorescence image (omitting myosin7a signal) of an $Rb^{-/-}$ cochlear whole mount from an apical turn on P5 displaying mitotic IHCs (arrowheads) and OHCs (arrows). Note an IHC in anaphase (two opposing arrowheads). Rows of OHC1, OHC2, and IHC are labeled based on DAPI and myosin7a staining (data not shown). (*G* and *H*) Confocal images of TUNEL-labeled (red, asterisk) cross-sections through the organ of Corti on P4. (*G*) $Rb^{+/-}$. (*H*) $Rb^{-/-}$. Blue, DAPI. Arrows and arrowheads indicate OHCs and IHCs, respectively. TUNEL-positive HCs were detected at presumed locations of IHCs (data not shown). (*I* and *J*) Confocal *z* projection of an $Rb^{-/-}$ apical cochlear whole mount on P6. Blue, DAPI; green, myosin7a. Arrowheads indicate kidney-shaped and abnormal, partially fragmented nuclei of HCs. (Scale bars: 10 μm.)

chromatin conformation in $Rb^{-/-}$ HC nuclei were revealed by 4′, 6-diamidino-2-phenylindole (DAPI) staining (Fig. 3*D*). In addition, HCs were rounding up, indicative of mitosis (Fig. 3*D*). High-resolution microscopy further identified mitotic HC nuclei based on morphologic features, such as the appearance of individual chromosomes in prophase (Fig. 3*E*). By counting such mitotic nuclei in two littermates on P4, we determined that ≈28% of HCs were in the M phase (Fig. 3 *E* and *F*). Thus, it is clear that ≈40% of HCs had reentered the cell cycle at P4. Mitotic cells were observed in basal and apical locations (Fig. 3 *E* and *F*). M phase entry of $Rb^{-/-}$ HCs generally correlated with the migration of the cell nucleus from a basal to a more apical subcellular location; consequently, these HCs did not align in the plane with "normal" HC nuclei (Fig. 3 *D–F*). Similar phenomena have been observed in normal dividing cells in the developing retina (17).

To characterize the HC death, we performed terminal transferase dUTP nick-end labeling (TUNEL), which detects breakage in nuclear DNA, characteristic for cells dying from apoptosis. On P4, weakly to brightly labeled OHC and IHC nuclei were observed, indicating early or late stages of apoptotic HC death (Fig. 3 *G* and *H*; data not shown). Scanning whole mounts of $Rb^{-/-}$ cochleae within the HC nuclear layer, we observed abnormal kidney-shaped and quasi-binucleated HC nuclei (Fig. 3*I*) and morphologically apoptotic HC nuclei (Fig. 3*J*). We found that the nuclei of SCs adjacent to dying HCs appeared unaltered morphologically and normally localized on P6 and P15 (data not shown), suggesting that HC loss did not immediately cause SC death.

Developmental Gradient of the HC Phenotype. We analyzed whole mounts of $Rb^{-/-}$ cochleae on P9, a stage when HCs are more mature, especially those in the basal turns. We still observed cell-cycle reentry on P9, with HCs rounding up and displaying nuclear migration (Fig. 4 *A* and *B*). Strikingly, it was only in the most apical tips of $Rb^{-/-}$ cochleae that we observed clusters of HCs containing up to four nuclei that were compacted and did not intermix with the cytoplasm and were incompletely compartmentalized (data not shown). Some clusters displayed symmetry (Fig. 4*C*), reminiscent of symmetric acytokinetic mitoses, consistent with HCs in later stages of mitosis occasionally observed within the apical region (Fig. 3*F*).

The OHC maturation marker prestin is normally expressed in the whole cell membrane by P7 and is almost completely absent from the apical and basal cell poles in later developmental stages (18, 19). In contrast to the complete lack of prestin expression in $Rb^{-/-}$ HC precursors (10), most OHCs in $Rb^{-/-}$ mice on P9 displayed the mature prestin expression pattern, but this pattern was abnormal in OHCs entering the cell cycle (Fig. 4).

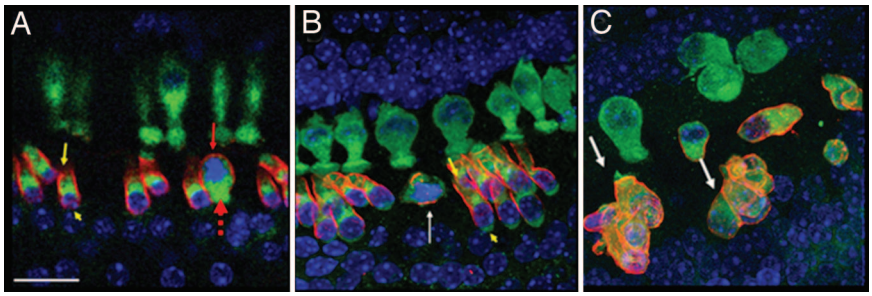

Fig. 4. HC clusters in the most apical cochlear turns and prestin expression. Confocal *z* projection of an $Rb^{-/-}$ cochlear whole mount on P9. Green, myosin7a; red, prestin; blue, DAPI. (*A*) Basal cochlear turn with significant HC loss. The dotted red arrow indicates a mitotic OHC that has rounded up, displaying nuclear migration. the yellow arrow and arrowhead indicate apical and basal poles, respectively, of an apparently normal OHC with the mature prestin expression pattern, which is reduced or absent at the apical and basal poles. The red arrow indicates the abnormal subcellular distribution of the membrane protein prestin in the same cochlear region. (*B*) Mid-apical cochlear turn. The white arrow indicates a rounded-up OHC next to apparently normal OHCs; the yellow arrowhead and arrow are as in *A*. Note that apical HCs are larger and display a more distinct prestin-free basal pole beginning at the supranuclear region. (*C*) Most apical cochlear tip. Note HC loss and OHC clusters (white arrows) with abnormal prestin expression. (Scale bars: 25 μm.)

Discussion

Roles of Rb in Various Phases of the Cell Cycle. In contrast to other studies in which germ-line or tissue-specific deletions of Rb or other cell-cycle regulators led to the gradual loss of HCs (2, 10, 20–22), our study showed that HC responses were rapid and fairly synchronized. Within 4–5 days after induction and 2–3 days after acute loss of *Rb* gene function, ≈40% of cochlear HCs (Fig. 3) had reentered the cell cycle, and ≈10% had already died (Fig. 2*E*), demonstrating the overriding role of Rb in maintaining the quiescence of postnatal HCs. With respect to the time course of cell-cycle reentry upon acute loss of Rb, our *in vivo* findings were strikingly similar to those of an *in vitro* study performed in mouse embryonic fibroblasts (23). In addition to controlling the G_1/S checkpoint, Rb plays various roles during the cell cycle (24–26). This is reflected by the presence of kidney-shaped and bilobed nuclei in some $Rb^{-/-}$ HCs. Although the vast majority of mitotic $Rb^{-/-}$ HCs we observed were in prophase, we also detected HCs in later stages (Fig. 3*F*). Thus, the absence of supernumerary HCs and the accumulation of HC clusters point to defects in completing cytokinesis. Cycling myocardiocytes have been shown to arrest at different stages, including mitosis and cytokinesis, and only a fraction underwent cell division, whereas, under certain insults, some postmitotic neurons reentered the S phase but died before the M phase (27). It remains open how inactivation of Rb triggers HC death in various phases of the cell cycle, as we observed, and experiments focused on cell-cycle- or apoptosis-associated Rb pathway genes will be necessary. Although other pocket domain proteins (e.g., p130 and p107) can compensate for specific functions of Rb (28–32), the dramatic phenotype observed in our study can be simply explained by the reported absence of other pocket domain proteins in postnatal HCs (2).

Responses to Rb Loss Depend on the Differentiation Stages of HCs. Responses to Rb loss in postnatal cochlear HCs are different from those in embryonic undifferentiated HC precursors. When Rb was absent before the cell-cycle exit, ongoing proliferation led to supernumerary HCs and SCs, some of which were functional and escaped death on E18.5 (2, 9). Such proliferation did not occur when Rb was inactivated in postnatal HCs, as shown in our study; instead, rapid cell-cycle reentry and subsequent cell death within all cochlear regions ensued. It is likely that the ablation of Rb in previous embryonic studies (9, 10) simply delayed cell-cycle exit, resulting in an increased number of hair cells, similar to the consequences of ablating several other cell-cycle regulators (20–22). It would therefore be interesting in the future to directly test whether the loss of Rb in early postmitotic, embryonic HC, and SC precursors at approximately E14 also causes cell-cycle reentry, leading either to rapid proliferation and generation of additional HCs and SCs (10) or to rapid cell death as reported here. Using a mouse model in which Rb had been deleted in the germ line, Mantela *et al.* (2) described increased apoptosis of Rb-null proliferating HC precursors at embryonic ages; we thus expect a similar outcome after acute inactivation at approximately E14.

Interestingly, we also observed variations of responses to Rb inactivation between basal and apical turns of the cochlea. HC clusters were observed in only the most apical tips of $Rb^{-/-}$ cochleae. During early postnatal development, apical HCs are less mature, resembling developing embryonic HCs, whereas basal HCs are more mature, resembling adult HCs (33). It appears that the least differentiated cells in our study, located in the apical tips, had undergone endoproliferation (acytokinetic mitosis) to form multinucleated clusters. In a previous study, similar multinucleated HCs were observed in late embryonic stages in germ line-mutated ($Rb^{-/-}$) mice (2). Despite this similarity, it remains possible that HC clusters observed in our study are fusion products of multiple dividing HCs and that this property is associated with only developmentally younger and less differentiated HCs. Our findings further support a "time window" for the generation of supernumerary HCs, as suggested in ref. 34. Interestingly, a trend toward earlier loss of OHCs is apparent, although not significant. It might reflect subtle differences between the two types of HCs with regard to their developmental stages and kinetics in response to the acute loss of Rb function. Alternatively, it might simply reflect slight differences between IHCs and OHCs regarding Cre activity (ref. 14 and Fig. 1*D*).

Roles of Rb in Postnatal HC Maturation. The presence of prestin in *Rb*-null OHCs in our model strongly suggests that Rb is not required during postnatal OHC maturation for the continued expression of prestin. However, prestin was completely absent in OHCs after Rb inactivation in early embryonic HC precursors (10). Again, these findings highlight the importance of developmental stages of HCs in their responses to Rb inactivation and suggest that Rb indirectly induces OHC-specific gene expression before the loss of Rb function induced in our study (i.e., before P2).

Implications for HC Regeneration Studies in Mice and Humans. Regenerating HCs by inactivating Rb or other cell-cycle regulators in residual postnatal HCs is a daunting task. Even if transient Rb inactivation in the remaining HCs were achieved, the cell surveillance machinery would have to be manipulated simultaneously to keep cells alive without immortalizing them. It

remains unknown whether the HCs in our study died from the loss of Rb gene function or from an age-dependent decline in proliferative ability. Our HC-specific, inducible Cre mouse model will be helpful to address this critical question by manipulating other cell-cycle regulators.

Inherited predisposition to the childhood malignancy retinoblastoma occurs in individuals carrying a germ-line mutation of one allele of *Rb* and loss of the second *Rb* allele through somatic mutation in retinoblastoma tumors (35). Hearing loss in children treated for this eye disease is associated with chemotherapy (36). Indeed, our model suggests that the loss of the second *Rb* allele in individual HCs would result in immediate cell-autonomous cell death, without affecting hearing function or causing dysplasia. A possible link between Rb and hearing disorders in humans is an autosomal-dominant auditory neuropathy, which has been mapped to chromosome 13 (37). The marker with the highest LOD score is localized in intron 2 of the *Rb* gene, suggesting that Rb is a candidate deafness gene in humans.

Materials and Methods

Mouse Models. $Rb^{lox/lox}$ mice (13) were kindly provided by A. Berns (The Netherlands Cancer Institute, Amsterdam, The Netherlands) through the National Cancer Institute Mouse Models of Human Cancers Consortium. The care and use of the mice during the course of this study were approved by the Institutional Animal Care and Use Committee at St. Jude Children's Research Hospital.

Tissue Preparation and DNA Isolation. Cochleae were dissected and processed as described in ref. 16. PCR primers and procedures used for genotyping and the application of tamoxifen were as described in refs. 38 (Rb) and 14 (Cre and lacZ).

Immunostaining, lacZ Staining and Microscopic Analysis. Antibodies against prestin (1:200; Santa Cruz), myosin7a (1:200; Proteus BioSciences), or phosphorylated Ser-10 of histone H3 (1:100; Abcam) and secondary antibodies (1:1,000; Alexa Fluor 594 or 488) were used. A fluorescence (Olympus) or a multiphoton (Zeiss LSM, Axioplan) microscope was used in confocal mode for imaging analysis. For high-resolution fluorescence microscopy, cryosections were treated with Carnoy's fixative (3 vol of absolute methanol and 1 vol of glacial acetic acid), washed in PBS, and stained with DAPI. Images were captured with a Nikon Labophot 2 microscope, using Metamorph software, Version 6.2r6, and were deconvoluted by using AutoDeblur software, Version X1.4.1 (Media Cybernetics). LacZ staining of cochleae was performed as described in ref. 14.

Hair Cell Counts. The numbers of IHCs and OHCs per 100 μm of whole mount length within specific turns were calculated and compared with those of littermates for each age group as a percentage ($Rb^{-/-}/Rb^{+/-}$). To prevent movements of the specimens during microscopic analysis, whole mounts were prepared by using a hardening medium (Vectashield HardSet with DAPI; Vector Laboratories). We chose a representative region within a specific cochlear turn and determined its length from within the inner row of OHCs, using LSM image browser software (Zeiss). The presence or absence of HCs was determined on the basis of two independent HC markers (prestin and myosin7a), using confocal microscopy. The length of the analyzed regions was 614.9 ± 61.0 μm ($n = 61$) containing 233.7 ± 26.0 OHCs ($n = 20$) and 71.4 ± 7.4 IHCs ($n = 22$) in $Rb^{+/-}$ mice.

Proliferation and TUNEL Staining. Undiluted BrdU labeling reagent (15 μl per gram of body weight; Roche) was used. Cryosections were stained with the myosin7a antibody and then treated with 2 N of HCl for 10 min at room temperature, washed three times in PBS and then in 0.1 M Tris (pH 8.0), washed again twice in PBS, and stained for BrdU (Roche). TUNEL staining was performed on cryosections, using reagents from the ApopTag red *in situ* apoptosis detection kit (Chemicon).

ACKNOWLEDGMENTS. We thank Drs. M. Dyer, B. Schwers, and K. Kitagawa for advice and for sharing reagents; Y. Tian for discussion; X. Wu for technical advice; and M. Roussel for critical comments. This work was supported in part by National Institutes of Health Grants DC06471, DC05168, DC008800, CA21765, CA023944, A096832, and NS044172; the Deafness Research Foundation; the Jean-François St.-Denis Fellowship in Cancer Research from the Canadian Institutes of Health Research; the American Lebanese Syrian Associated Charities of St. Jude Children's Research Hospital; and a Hartwell Individual Biomedical Research Award (J.Z.).

1. Lee YS, Liu F, Segil N (2006) *Development (Cambridge, UK)* 133:2817–2826.
2. Mantela J, Jiang Z, Ylikoski J, Fritzsch B, Zacksenhaus E, Pirvola U (2005) *Development (Cambridge, UK)* 132:2377–2388.
3. Ruben RJ (1967) *Acta Otolaryngol*, 220(Suppl):1–44.
4. Kelley MW (2006) *Brain Res* 1091:172–185.
5. Corwin JT, Oberholtzer JC (1997) *Neuron* 19:951–954.
6. Ryals BM, Rubel EW (1988) *Science* 240:1774–1776.
7. Taylor RR, Forge A (2005) *J Comp Neurol* 484:105–120.
8. Sherr CJ (2000) *Cancer Res* 60:3689–3695.
9. Sage C, Huang M, Karimi K, Gutierrez G, Vollrath MA, Zhang DS, Garcia-Anoveros J, Hinds PW, Corwin JT, *et al.* (2005) *Science* 307:1114–1118.
10. Sage C, Huang M, Vollrath MA, Brown MC, Hinds PW, Corey DP, Vetter DE, Chen ZY (2006) *Proc Natl Acad Sci USA* 103:7345–7350.
11. Wikenheiser-Brokamp KA (2006) *Cell Mol Life Sci* 63:767–780.
12. Nagy A (2000) *Genesis* 26:99–109.
13. Marino S, Vooijs M, van Der Gulden H, Jonkers J, Berns A (2000) *Genes Dev* 14:994–1004.
14. Chow LM, Tian Y, Weber T, Corbett M, Zuo J, Baker SJ (2006) *Dev Dyn* 235:2991–2998.
15. Soriano P (1999) *Nat Genet* 21:70–71.
16. Wu X, Gao J, Guo Y, Zuo J (2004) *Brain Res Mol Brain Res* 126:30–37.
17. Pearson RA, Luneborg NL, Becker DL, Mobbs P (2005) *J Neurosci* 25:10803–10814.
18. Weber T, Zimmermann U, Winter H, Mack A, Kopschall I, Rohbock K, Zenner HP, Knipper M (2002) *Proc Natl Acad Sci USA* 99:2901–2906.
19. Winter H, Braig C, Zimmermann U, Geisler HS, Franzer JT, Weber T, Ley M, Engel J, Knirsch M, Bauer K, *et al.* (2006) *J Cell Sci* 119:2975–2984.
20. Chen P, Segil N (1999) *Development (Cambridge, UK)* 126:1581–1590.
21. Chen P, Zindy F, Abdala C, Liu F, Li X, Roussel MF, Segil N (2003) *Nat Cell Biol* 5:422–426.
22. Lowenheim H, Furness DN, Kil J, Zinn C, Gultig K, Fero ML, Frost D, Gummer AW, Roberts JM, Rubel EW, *et al.* (1999) *Proc Natl Acad Sci USA* 96:4084–4088.
23. Sage J, Miller AL, Perez-Mancera PA, Wysocki JM, Jacks T (2003) *Nature* 424:223–228.
24. Hernando E, Nahle Z, Juan G, Diaz-Rodriguez E, Alaminos M, Hemann M, Michel L, Mittal V, Gerald W, Benezra R, *et al.* (2004) *Nature* 430:797–802.
25. van Deursen JM (2007) *Cancer Cell* 11:1–3.
26. Zacksenhaus E, Jiang Z, Chung D, Marth JD, Phillips RA, Gallie BL (1996) *Genes Dev* 10:3051–3064.
27. Bettencourt-Dias M, Mittnacht S, Brockes JP (2003) *J Cell Sci* 116:4001–4009.
28. Chen D, Livne-bar I, Vanderluit JL, Slack RS, Agochiya M, Bremner R (2004) *Cancer Cell* 5:539–551.
29. Donovan SL, Schweers B, Martins R, Johnson D, Dyer MA (2006) *BMC Biol* 4:14.
30. MacPherson D, Sage J, Kim T, Ho D, McLaughlin ME, Jacks T (2004) *Genes Dev* 18:1681–1694.
31. Robanus-Maandag E, Dekker M, van der Valk M, Carrozza ML, Jeanny JC, Dannenberg JH, Berns A, te Riele H (1998) *Genes Dev* 12:1599–1609.
32. Zhang J, Gray J, Wu L, Leone G, Rowan S, Cepko CL, Zhu X, Craft CM, Dyer MA (2004) *Nat Genet* 36:351–360.
33. Rubel EW, Born DE, Deitch JS, Durham D (1984) in *Hearing Science: Recent Advances*, ed Berlin CI (College-Hill Press, San Diego), pp 109–157.
34. Kelley MW, Xu XM, Wagner MA, Warchol ME, Corwin JT (1993) *Development (Cambridge, UK)* 119:1041–1053.
35. Laurie NA, Donovan SL, Shih CS, Zhang J, Mills N, Fuller C, Teunisse A, Lam S, Ramos Y, Mohan A, *et al.* (2006) *Nature* 444:61–66.
36. Lambert MP, Shields C, Meadows AT (2008) *Pediatr Blood Cancer* 50(2):223–226.
37. Kim TB, Isaacson B, Sivakumaran TA, Starr A, Keats BJ, Lesperance MM (2004) *J Med Genet* 41:872–876.
38. Vooijs M, van der Valk M, te Riele H, Berns A (1998) *Oncogene* 17:1–12.